

interpretation of data, in the writing of the report, or in the decision to submit the paper for publication.

I believe that the article is suitable for publication in your journal because we describe successfully the incorporation of two different titanates (nanosheets and nanotubes) inside the pores of anodized TiO₂ nanotubes array using an electrophoretic deposition method. Furthermore, this study demonstrates that the mechanical stimulation of the counter electrode equipped with a brush avoided the accumulation of a thick outer layer on the TiO₂ nanotubes. We believe that our work is novel because, as far as we are aware, no reports are available concerning this hierarchical structure involving titanates and TiO₂ nanotubes and the relationship with improvement in properties as surface area, hydrophobicity and electrical conductivity.

We look forward to hearing from you concerning our submission in due course.

Yours sincerely,

Marcos R. V. Lanza

INSERTION OF NANOSTRUCTURED TITANATES INTO THE PORES OF AN ANODISED TiO₂ NANOTUBE ARRAY BY MECHANICALLY STIMULATED ELECTROPHORETIC DEPOSITION

Alysson S. Martins^{a,b*}, Christian Harito^a, Dmitry V. Bavykin^a, Frank C. Walsh^a, Marcos R. de V. Lanza^b.

^a *Energy Technology Research Group, Faculty of Engineering and the Environment, University of Southampton, UK.*

^b *Instituto de Química de São Carlos, Universidade de São Paulo, Avenida Trabalhador São-Carlense 400, São Carlos, SP, 13566-590, Brazil.*

- *correspondence author:* marcoslanza@iqsc.usp.br

Key words: nanostructured titanates, abrasion, hierarchical, nanoarchitecture, nanoparticle.

Introduction

TiO₂ has seen renewed interest over the last three decades due to its wide range of applications in chemistry/engineering [1] as a photocatalyst [2], in sensors [3], as self-cleaning surfaces [4], for hydrogen evolution cathodes [5], in corrosion protective coatings [6] and as a bactericide [7]. TiO₂ can be applied in such diverse areas due to its distinct chemical properties, which include chemical resistance over a wide pH, low toxicity and appropriate redox potential to catalyse different reactions [8]. In particular, TiO₂ morphologies based on nanotubes - TiO₂NT- have become attractive in synthesis due to their ability to generate precise structures having controlled pores and walls with a varied inner diameter [8]. Various studies have involved changes in TiO₂NT semiconductors in order to improve its performance [9,10,11]. The modifications generally aim to cover the TiO₂ with other materials for increase the specific surface area, decrease in electron/hole recombination and improve stability [12,13,14,15].

Among modified structures, titanates have attracted a great deal of attention, especially when combined with TiO₂ semiconductors. Typically, titanates are multiple H₂Ti₃O₇ structures that present random nanotubular morphology and may be modified with other metallic oxides [16,17,18]. Their dispersion in TiO₂ matrices can enable a considerable increase in surface area and rapid transport through the porous network. The choice of such materials is primarily due to the simplicity of synthesis and the ease with which the surface can be modified. Our group has successfully fabricated titanates under hydrothermal treatment and by sol-gel with formation of particular nanostructures including nanotubes, TiNT and nanosheets, TiNS that provide extra surface area and greatly facilitate absorption [18].

The insertion of titanates in a TiO₂NT matrix can be commonly performed by such coating technologies as hydrothermal deposition [19], sol-gel [20], chemical and physical vapour deposition, electrospinning [21,22] and, more recently, electrophoretic deposition – EPD [23,24]. The EPD technique involves an electrolyte prepared by dispersing colloidal particles in an aqueous solution followed by their controlled migration under the influence of an electric field (electrophoresis) to be deposited onto the electrode surface [25]. This technique has been studied due to ease of handling, versatility, simplicity and low cost. It presents advantages over other techniques such as chemical vapour deposition which can involve extreme conditions of temperature and pressure together with limited chamber shape and size.

In the case of titanates and TiO₂NT, the main advantage of EPD is easy control of the thickness of the deposited through adjustment of the time and applied potential [26,27,28]. Even with the control of such variables, most incorporations are limited to the outer surface of the electrode. Although there have been numerous studies of EPD, the deposition in more complex structures as pores of TiO₂ nanotubes have not been successfully realized. The results reported have provided decrease the surface area of TiO₂ nanotubes [29,30] and a low efficiency of transport through the porous network. This panorama requires the development of a new method for deposition of titanates inside of macropore of TiO₂NT. The present study reports a novel incorporation of TiNT and TiNS in the macropores of TiO₂NT using a brush-assisted stimulation of the surface during electrophoretic deposition.

In this work, three different syntheses of TiO₂ were explored; the nanotube array TiO₂-NT which was produced by electrochemical anodising, titanate nanotubes, TiNT were

produced via hydrothermal treatment and titanate nanosheets, TiNS were achieved via a sol-gel process. To promote insertion of TiNT and TiNS in TiO₂-NT by EPD, it was necessary to develop a mechanically-assisted electrochemical process. Figure 1(A) schematically shows a horizontal plate of TiO₂-NT where the surface is drip irrigated by a colloidal solution of titanates. The applied potential associated with short distance between working and counter electrode favours the migration of negatively charged titanate particles toward the positively charged TiO₂NT plate. The counter electrode is manually moved over the surface of TiO₂NT to avoid bulk deposition of TiNT or TiNS on the outer surface of the working electrode. This work provides an improved method to successfully deposit titanates deep inside the macropores of TiO₂TN via EPD.

Experimental Details

The sol-gel synthesis of TiNS [31] involved modification of a titanium precursor. 10 mL of titanium n-butoxide was added slowly to 150 mL of aqueous solution of 0.273 M tetramethylammonium hydroxide (TMAOH) and stirred for 5 minutes at room temperature (25 °C). The mixture was refluxed under argon at 95 °C for 24 h. The solution was turbid on addition of titanium n-butoxide but slowly became transparent after 30 minutes. After 6 h, it became opaque and remained so after the reaction.

TiNT were prepared by the alkaline hydrothermal method [18]. 10 mol L⁻¹ of KOH:NaOH 1:25 was mixed with 25 g TiO₂ (Degussa P25). The solution was stirred and kept under reflux for 2 days at 100 °C. The white clusters generated were washed several times to achieve pH 7. To convert the TiNT to their protonated form, the white powder was washed with 0.1 mol L⁻¹ HCl until the rinse solution stabilised at pH, washed with water to achieve pH 5 then dried overnight at 140 °C under ambient air conditions.

The titanium (Ti) foil (99% purity, 1 mm thickness and $2.4 \times 2.4 \text{ cm}^2$ area) used for growth of TiO_2NT was previously polished with SiC paper of successively finer particle sizes of 320, 400, 800 and 1200 grit. The foils were cleaned in isopropyl alcohol, acetone and ultrapure water ($1.3 \mu\text{S cm}^{-1}$) in an ultrasonic bath for 5 minutes then dried under N_2 gas. Anodizing was performed in a cell containing a titanium plate anode and a planar stainless steel cathode at a distance of 1 cm. The electrolyte used was 0.3 % HF and 1 M NaH_2PO_4 in aqueous solution. The applied potential was increased by 1 V every 30 seconds to arrive at 20 V then held constant for 2 hours using a smooth DC power supply [32]. The electrodes were washed with ultrapure water, dried with N_2 gas then calcinated at $450 \text{ }^\circ\text{C}$ for 2 hours at a linear heating rate of $2 \text{ }^\circ\text{C min}^{-1}$.

Electrophoretic deposition of TiNS/TiNT was performed in the system shown in Figure 1. A suspension of 100 mg L^{-1} TiNT was previously immersed in an ultrasonic bath for 3 hours to decrease the average nanotube length; this procedure facilitated the penetration of TiNT on TiO_2NT . The EPD was carried out onto the surface of TiO_2NT ($2.4 \times 2.4 \text{ cm}^2$) where was added 1 cm^3 of the electrolyte containing 5% (v/v) of the titanate suspension (TiNS or TiNT) dispersed in methanol-water (50:50, vol.); the conductivity resultant was 859 and $5 \mu\text{S cm}^{-1}$ to TiNS and TiNT electrolyte, respectively. The $\text{TiO}_2\text{-NT}$ Ti anode and the stainless steel cathode were kept parallel at distance of 0.5 mm to maintain a thin-film electrolyte thickness of 0.5 mm on the surface. The anodic potential applied to the cell was 20 V over 20 minutes at $25 \text{ }^\circ\text{C}$. To avoid blocking the surface of $\text{TiO}_2\text{-NT}$ with titanates, a modified brush, which consists of nylon bristles, was used near the counter electrode. Figure 1 shows a schematic of the arrangement and the expected behavior; the movement of the counter electrode in the

electrolyte prevents formation of a compact layer of titanates on the surface of TiO₂NT. The titanates can then be incorporated inside the pores in the presence of the potential gradient.

The morphology of the samples was evaluated by SEM using a JSM 6500F thermal emission scanning electron microscope - SEM, operating at an accelerating voltage of 15 kV. Raman spectra of the electrodes were collected using a Renishaw 2000 spectrometer with HeNe laser ($\lambda = 632.8$ nm) excitation. The surface hydrophobicity was determined by measuring the water contact angle (WCA) using a WCA analyzer (DigiDrop MCA, GBX).

Electrochemical measurements were carried on an electrochemical workstation (IviumStat.h) in a three-electrode system, using the TiO₂NT on Ti as a working electrode, platinum foil as a counter electrode and SCE as a reference electrode. Cyclic voltammetry was performed in 0.1 mol L⁻¹ Na₂SO₄ and 0.025 mol L⁻¹ Methylene Blue, MB in 0.1 mol L⁻¹ Na₂SO₄ at a linear scan rate of 20 mV s⁻¹ over the potential range from -1.0 V to +1.0 V vs. SCE.

Results and Discussion

Multihierarchical electrode characterisation

The morphology of materials synthesized was evaluated via SEM, the Figure 2(A) shows titanates nanosheets, TiNS ordered with structures well-defined, rectangular outline and good regularity of size with average length of 20 nm. The titanates nanotubes in Figure 2(b) are clustered with a high surface area and length suited to the EPD technique. In order to reduce their size, they were sonicated for 3 h in a colloidal

suspension generating nanotubes 70-100 nm in diameter, as shown in the inset of Figure 2(b).

The TiO₂-NT produced by electrochemical anodising, Figure 2(c), revealed good linearity and periodicity of nanotubes with a diameter of 90-110 nm and tube wall thickness of *ca.* 10 nm. The cross-section in Figure 2(d) shows a highly ordered nanotube array perpendicular to the Ti substrate with an average length of 800 – 900 nm. The uniform lengths of these materials make them potential candidates as substrates in EPD studies. The nanosheets and nanotubes are small enough to be inserted inside the large TiO₂ pores.

In order to compare the efficiency of EPD synthesis, two different depositions were previously performed in the TiO₂NT. To the first, the nanosheets suspension was deposited directly in the surface of TiO₂NT without potential application which was called TiNS/TiO₂NT-drop. The Figure 3(a) shows SEM images of the electrode where the top-view present nanotube with TiNS uniformly deposited on the surface. The top entrances of nanotubes are not discernible, since they are covered by TiNS. The TiNS are not successfully incorporated within pores but only on the outer surface. As a result, there is a decrease of surface area and also a possible decrement of light harvesting ability.

To the second deposition the TiNS was deposited in the TiO₂NT via EPD, referred to as TiNS/TiO₂NT-EPD; the EPD system is shown schematically in Figure 1(b). The SEM image in Figure 3(b) reveals an ultrathin and translucent layer of TiNS uniformly deposited on the surface of TiO₂NT. Due to the thin and superficial deposition, this

layer was not sufficiently stable for further characterization. It should be noted, however, that the TiNS is thinner compared to the first in which the TiNS are thicker on the top of entrances of TiO₂NT. The applied potential and movement of the counter electrode contributed to a uniform distribution of TiNS on the TiO₂ surface.

The influence of the brush modified counter electrode in EPD (EPDmod) was subsequently evaluated. As shown in Figure 1(c) and 1(d), this adaptation can facilitate insertion of titanates inside the pores due to movement of the brush across the surface. Both TiNS and TiNT were evaluated via EPDmod where electrodes modified were called TiNS/TiO₂NT-EPDmod and TiNT/TiO₂NT-EPDmod, respectively. The results for deposition show that the surface of TiO₂NT was completely covered by TiNS in Fig. 3(c) as well as TiNT in Fig. 3(d). Indeed, there is no layer of titanates covering the surface of TiO₂NT; the TiNS and TiNT are inside of the pores of nanotubes that present empty and full cavities, well distributed. The modification with TiNS and TiNT via EPD-mod increases the surface area of the electrode and improves the short circuit current for electrocatalytic applications. These results clearly confirmed the successful incorporation of titanates properly inside the nanotubes and the importance of EPD to achieve insertion of nanomaterials on more complex surfaces.

Raman spectroscopy was deployed to discriminate different crystalline states of titanium oxides on the electrodes. The spectra of all electrodes are shown in Figure 4. Prior to modification, they were subjected to thermal treatment (450 °C). The electrode of TiO₂NT before thermal treatment (TiO₂NT-amorphous) shows no peaks, indicating an amorphous structure. After thermal treatment, the diffraction pattern for the unmodified electrode (TiO₂NT-calcinated) and for all modified electrodes does not

differ significantly; they present similar peaks at *ca.* 147, 394, 518 and 637 cm^{-1} , characteristic of the anatase phase of TiO_2 [33,34]. It has been shown that the modification with TiNS/TiNT has not changed the structure of the electrodes. Particularly, the deposit on the nanotubes (800 nm) is relatively thin compared to the 1.5 mm thickness of the Ti metal substrate which can affect the evaluation of modifier in the surface of electrode.

However, the inset of Figure 4 shows a slight shift of peak at *ca.* 147 cm^{-1} which increased from 146.26 cm^{-1} of TiO_2 unmodified to 146.50 and 146.93 cm^{-1} to modification with TiNT and TiNS via EPD-mod, respectively. Moreover, there is a slight increase in the frequency of this peak from electrode of TiO_2 unmodified to electrodes modified via EPD. Both effects indicate that crystallinity was enhanced after modification due to bonding between the titanates and TiO_2 . Previous studies [35,36] indicate that this slight shift at *ca.* 147 cm^{-1} can be caused by the introduction of dopant atoms, which disturb Ti–O–Ti bonds and generate oxygen vacancies.

The wettability and water contact angle of the electrodes are summarized in the Figure 4. The electrodes unmodified revealed changes significant in the wetting properties. After thermal treatment in Fig. 4(a) the electrode became superhydrophilic ($\theta = \text{ca. } 16$ deg) in contrast to the originally super-hydrophobic surface before treatment as seen in the inset of Fig. 4(a). In general the surface wettability is governed by both the geometrical structure roughness and the chemical composition of the materials. In this case, the hydrophobicity increases with the annealing temperature which may change the oxygen vacancies. According to Zhang *et al.* [37] such a change may be due to

hydroxyl groups produced on the surface of the TiO₂-NT after calcination, which increase polar interactions with water.

After modification via EPD-mod the flat TiO₂ surface shows appreciable hydrophobicity with contact angle of \approx 33 deg and 39 deg for TiNS and TiNT electrodes, respectively. The change of hydrophilic to hydrophobic can improve the properties of electrodes for electrocatalytic applications, since the surface increases the adsorption capacities of organic compounds. Furthermore, the electrode with hydrophobic properties can avoid competition of adsorption of water molecules on the surface; in other words, adsorbents with non-polar properties such as organic molecules may facilitate their interactions in the surface.

Electrochemical studies

Cyclic voltammetry was performed to characterize the materials in contact with electrolyte (pH = 7). All electrodes showed capacitive and faradaic currents characteristic of the anatase electrodes in Figure 6. The anodic region (i) presents a low capacitive current while the cathodic region (ii) shows well developed peak couple ascribed to the Ti(III)/Ti(IV) in the TiO₂ sites [38].

Interestingly from the CV curves, the electrode TiO₂NT-calcinated shows only the cathodic peak in Fig. 6(a) while the TiNS/TiO₂NT-EPDmod and TiNT/TiO₂NT-EPDmod show both anodic and cathodic peaks in Fig. 6(c) and (d). These results are in good agreement with CV profiles of other works [39] and supported the behavior of TiO₂-NT and titanates. Electrodes of TiO₂-NT modified with titanates present double

peaks and are result of different orientations (001) and (101) of the titanates which show different flatband potentials.

Moreover, electrodes modified via EPD in Fig. 6(c) and (d) show more pronounced peaks compared to TiO₂NT-calcinated in Fig. 6(a). The incorporation of TNT certainly generates a change in the electronic structure of TiO₂ with generation of additional levels in the bandgap energy that consequently affects the electrical conductivity. In opposition, the electrode TiNS/TiO₂NT-drop in Fig. 6(b) shows a decrease of the current as well as disappearance of the peaks. In this case, the surface of TiO₂ nanotube is completely covered with nanosheets which blocks Ti⁴⁺ sites in TiO₂ and reduce the number of reactions at the interface. To more negative potential is initiated the hydrogen evolution process, reducing the current considerably.

Methylene blue, MB with a redox potential ($E^{\circ}_{redox} = 10$ mV) being more negative than the anatase flatband potential, was chosen as a redox indicator. During scanning (Figure 7) in the positive direction from -1.0 to 1.0 V a redox couple (dashed circles i and ii) can be observed. Comparing the same region with CVs in the blank solution (Figure 6) the peaks are associated with direct electrochemical oxidation of MB in the surface of electrodes, since the oxidation of MB and oxygen evolution are in significantly different potential regions. The electrodes modified via EPD show well developed redox peaks in Fig.7(d) and enlargement peaks in Fig.7(c), while the electrode TiNS/TiO₂NT-EPDdrop in Fig.7(b) show no significant peaks associated with MB oxidation. The TiO₂NT-calcinated electrode in Fig.7(a) shows the redox peaks of MB but their size is lower than the modified electrodes. This indicates that the two electrodes modified via EPD-mod had a higher direct oxidation capacity. The incorporation of titanates can change

the TiO₂ nanotube (anatase phase) surface states, which play an important role in the process of electrons transfer, and as intermediate states for electron transfer to the acceptor species in the electrolyte.

CONCLUSIONS

A novel method has been used to insert titanates into an anodized TiO₂ nanopore array via electrophoretic deposition. The incorporation of nanosheets in the absence of a potential gradient showed a higher nanosheet thickness on the top of TiO₂-NT. The application of a potential enabled robust deposition of titanates on the surface. Clearly, movement of the counter electrode over the surface of TiO₂-NT reduced the thickness of TiNS/TiNT layer in the surface, distributing them more homogeneously. More importantly, we describe the beneficial effect of adaptation in the counter electrode where firstly was avoided formation of the blocking deposits at the entrance of the TiO₂-NT. In other words, the titanates were inserted inside of the pores of nanotubes. Secondly, the modification via EPD-mod enhanced the surface area of the electrode and subsequently increase the short circuit current for electrocatalysis. Our results confirm that titanates can be readily deposited onto TiO₂ nanotube pores via electrophoretic deposition with an increased surface area, avoiding formation of a compact, bulk layer on the outer surface.

The hydrophobicity of the electrode surface became higher after modification by titanates. They could effectively avoid competition in the adsorption of water molecules on the surface. Cyclic voltammetry showed that the electrodes modified via EPD-modified assisted surface treatment showed higher currents with better direct oxidation capacity compared with pure TiO₂-NT and TiO₂ modified with surface nanosheets.

ACKNOWLEDGMENTS

The authors are grateful to São Paulo Research Foundation (FAPESP), grants #2013/08543-3, #2015/08815-9 and #2016/01937-4, Conselho Nacional de Desenvolvimento Científico e Tecnológico (CNPq), grant #301492/2013-1, and Coordenação de Aperfeiçoamento de Pessoal de Nível Superior (Capes) for financial support for this research.

REFERENCES

1. X. Li, J. Yu, J. Low, Y. Fang, J. Xiao and X. Chen, *J. Mater. Chem. A*, **3**, 2015, 2485-2534.
2. R. Dagherir, P. Drogui and D. Robert, *Ind. Eng. Chem. Res.*, **52**, 2013, 3581-3599.
3. Z. Lou, F. Li, J. Deng, L. Wang and T. Zhang, *ACS Appl. Mater. Interfaces*, **5**, 2013, 12310-12316.
4. Q. Xu, Y. Liu, F. Lin, B. Mondal and A. Lyons, *ACS Appl. Mater. Interfaces*, **5**, 2013, 8915-8924.
5. J. Priebe, J. Radnik, A. Lennox, M. Pohl, M. Karnahl, D. Hollmann, K. Grabow, U. Bentrup, H. Junge, M. Beller, and A. Brückner, *ACS Cat.*, **5**, 2015, 2137-2148.
6. M. Mahmoudian, Y. Alias, W. Basirun and, M. Ebadii, *Appl. Surf. Sci.*, **268**, 2013, 302-311.
7. T. Yuranova, A. Rincon, C. Pulgarin, D. Laub; N. Xantopoulos, H. Mathieu and J. Kiwi, *J. Photochem. Photobiol. A*, **181**, 2006, 363-369.
8. D. V. Bavykin, J. M. Friedrich and F. C. Walsh. *Adv. Mater.*, **18**, 2006, 2807-2824.
9. J. S. Souza, W. M. Carvalho, F. L. Souza, C. Ponce-De-Leon, D. V. Bavykin and W. A. Alves, *J. Mater. Chem. A*, **4**, 2016, 944-952.
10. S. Kang, J. Kim, Y. Kim, H. Kim and Y. Sung, *J. Phys. Chem. C*, **111**, 2007, 9614-9623.
11. A. Mohamed and S. Rohani, *Energ. Environ. Sci.*, **4**, 2011, 1065-1086.

12. K. Huo, B. Gao, J. Fu, L. Zhao and P. Chu, *RSC Adv.*, **4**, 2014, 17300-17324.
13. A. L. Stepanov, *Rev Adv. Mater. Sci.*, **30**, 2012, 150-165.
14. G. K. Mor, O. K. Varghese, M. Paulose, K. Shankar and C. A. Grimes, *Sol. Energ. Mat. Sol. Cells*, **90**, 2006, 2011-2075.
15. H. Park, Y. Park, W. Kim and W. Choi, *J. Photochem. Photobiol. C: Photochem. Rev.*, **15**, 2013, 1-20.
16. A. Jeffery, A. Pradeep and M. Rajamathi, *Phys. Chem. Chem. Phys.*, **18**, 2016, 12604-12609.
17. D. V. Bavykin and F. C. Walsh, *Eur. J. Inorg. Chem.*, **8**, 2009, 977-997.
18. D. V. Bavykin, A. N. Kulak and F. C. Walsh, *Cryst. Growth Des.*, **10**, 2010, 4421-4427.
19. T. Morita and Y. Cho, *Appl. Phys. Lett.*, **88**, 2006, 112908.
20. Y. Xing and X. Ding, *J. Appl. Polym. Sci.*, **103**, 2007, 3113-3119.
21. Q. Chen and L. Peng, *Int. J. Nanotechnol*, **4**, 2007, 44-65.
22. Y. Zhang, Z. Jiang, J. Huang, L. Lim, W. Li, J. Deng, D. Gong, Y. Tang, Y. Lai And Z. Chen, *RSC Adv.*, **5**, 2015, 79479-79510.
23. D. V. Bavykin, L. Passoni and F. C. Walsh, *Chem. Commun.*, **49**, 2013, 7007-7009.
24. S. Cabanas Polo and R. A. Boccaccini, *J. Eur. Ceram. Soc.*, **36**, 2016, 265-283.
25. L. Besra and M. Liu, *Prog. Mater Sci.*, **52**, 2007, 1-61.
26. A. Rabani and M. Noorsuhana, *BEIAC*, 2013, 56-60.
27. W. Sugimoto, O. Terabayashi, Y. Murakami and Y. Takasu, *J. Mater. Chem. A*, **12**, 2002, 3814-3818.
28. S. Radice, P. Kern, H. Dietsch, S. Mischler and J. Michler, *J. Colloid Interface Sci.*, **318**, 2008, 264-270.
29. X. Luan, L. Chen, J. Zhang, G. Qu, J. C. Flake, and Y. Wang, *Electrochim. Acta*, **111**, 2013, 216-222.
30. Y. Ji, *RSC Adv.*, **4**, 2014, 40474-40481.
31. E. Tae, K. Lee, J. Jeong and K. Yoon, *J. Am. Chem. Soc.*, **130**, 2008, 6534-6543.
32. A. Ghicov, B. Schimidt, J. Kunze and P. Schmukii, *Chem. Phys. Lett.*, **433**, 2007, 323-326.

33. X. Zhang, B. Yao, L. Zhao, C. Liang, L. Zhang and Y. Mao, *J. Electrochem. Soc.*, **148**, 2001, G398-G400.
34. J. Shen, H. Wang, Y. Zhou, N. Ye, G. Li and L. Wang, *RSC Adv.*, **2**, 2012, 9173-9178.
35. B. Choudhury, M. Dey and A. Choudhury, *Int. Nano Lett.*, **3**, 2013, 1-8.
36. K. Siuzdak, M. Szkoda, M. Sawczak, A. Lisowska-Oleksiak, J. Karczewski and J. Ryl, *RSC Adv.*, **5**, 2015, 50379-50391.
37. M. Zhang, G. Yao, Y. Cheng, Y. Xu, L. Yang, J. Lv, S. Shi, X. Jiang, G. He, P. Wang, X. Song and Z. Sun, *Appl. Surf. Sci.*, **356**, 2015, 546-552.
38. H. Pelouchova, P. Janda, J. Weber and L. Kavan, *J. Electroanal. Chem.*, **566**, 2004, 73-83.
39. M. Yarali, E. Bicer, S. Gursel and A. Yurum, *Nanotechnology*, **27**, 2016, 015401.

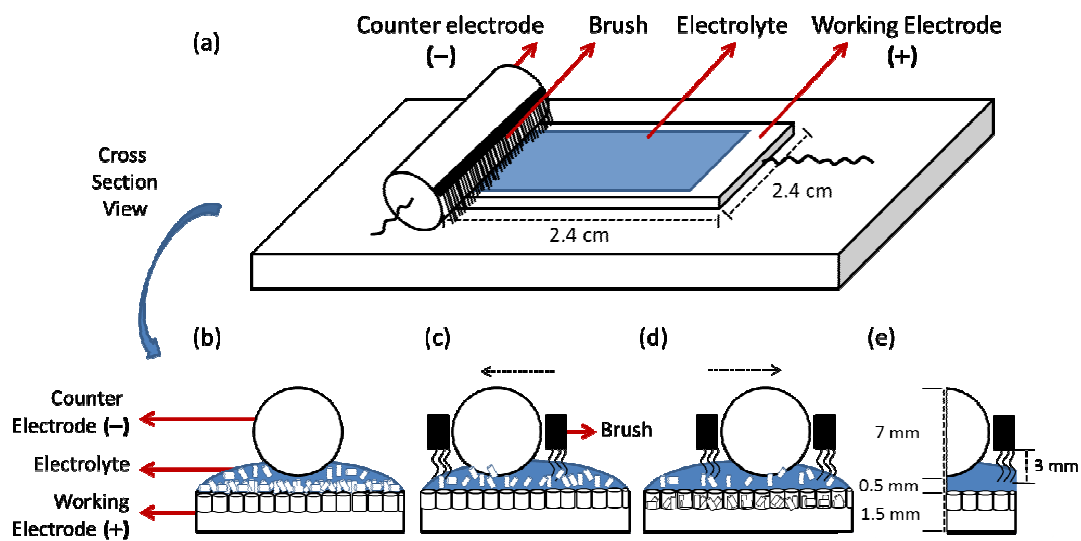


Figure 1: Schematic of electrophoretic deposition of titanates into the pores of TiO₂-NT using a brush modified surface treatment (a); generating compact layer of titanates in the substrate of TiO₂ nanotubes (b); brush moving the titanates in the surface (c); incorporation of titanates inside of pores of the TiO₂ substrate (d) and dimensions of the system (e).

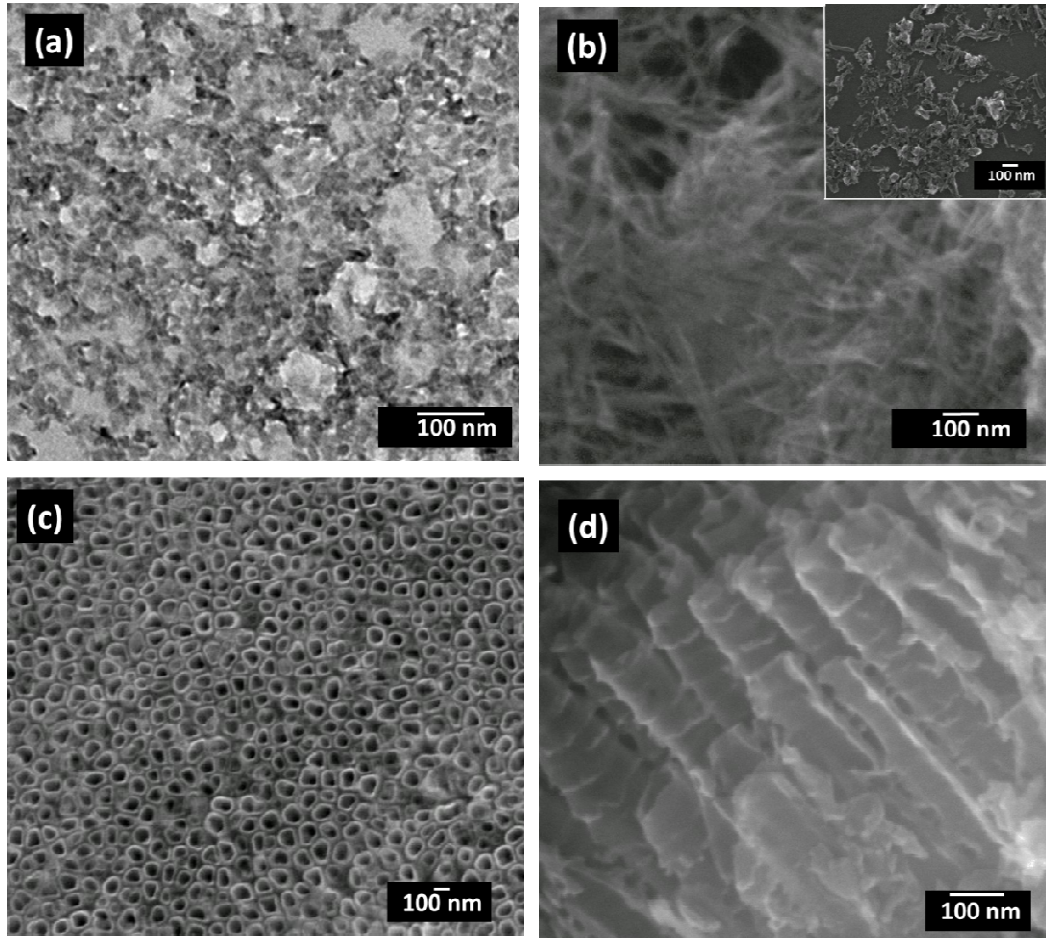


Figure 2: SEM images of TiNS (a); TiNT (b); top view (c) and cross section (d) of TiO₂NT.

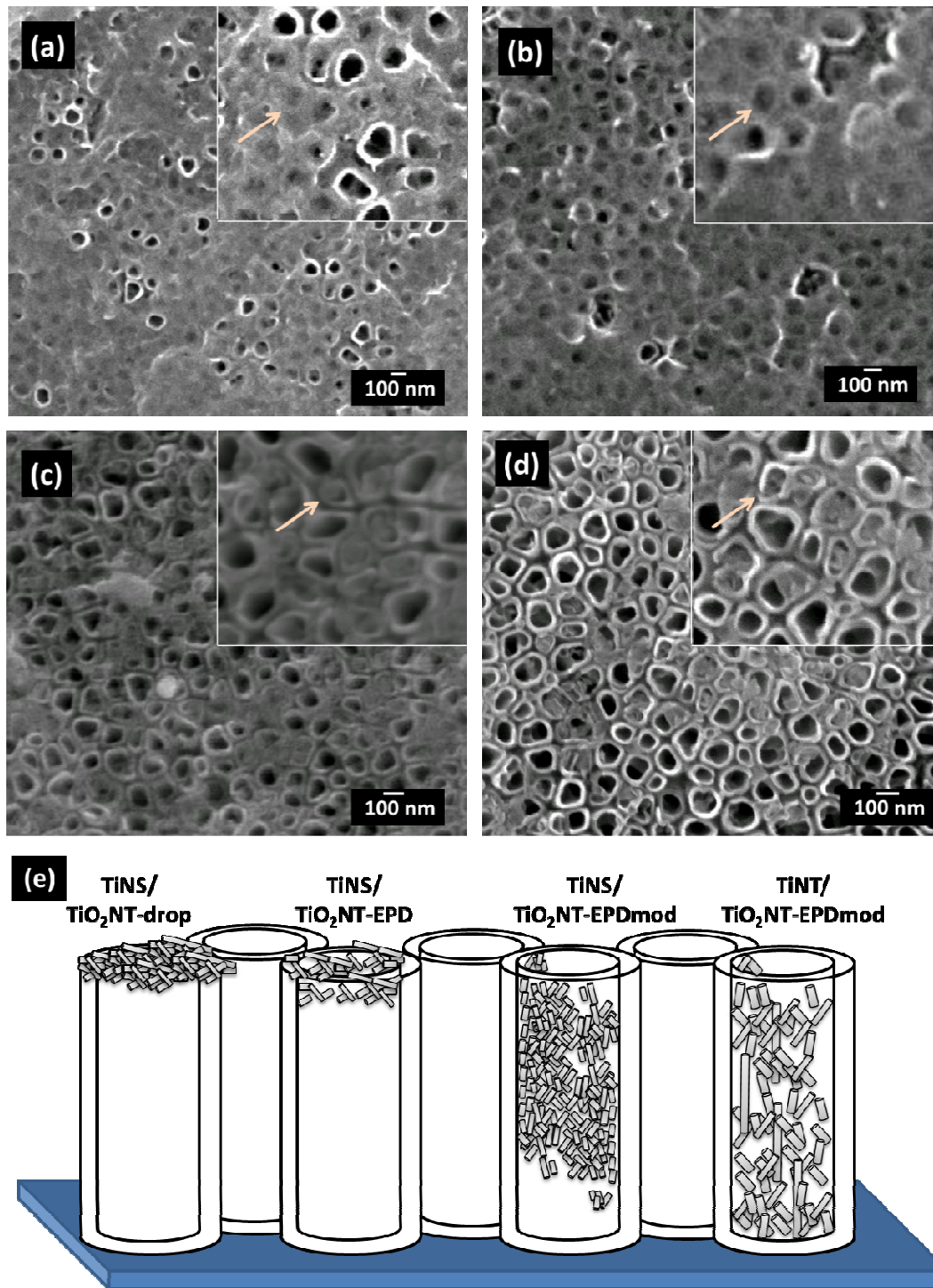


Figure 3: SEM images of (a) TiNS/TiO₂NT-drop; (b) TiNS/TiO₂NT-EPD; (c) TiNS/TiO₂NT-EPDmod and (d) TiNT/TiO₂NT-EPDmod. The pores indicated by the arrows in the insets are schematically represented in (e).

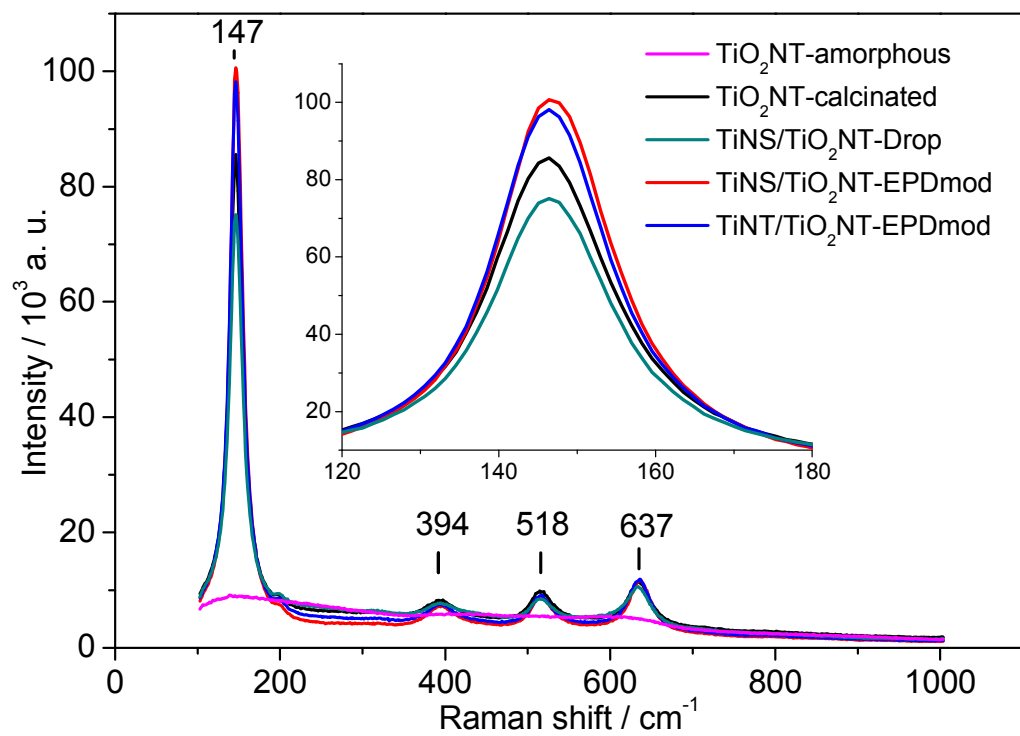


Figure 4: Raman spectra of TiO₂ nanotubes unmodified and modified with TiNT and TiNS.

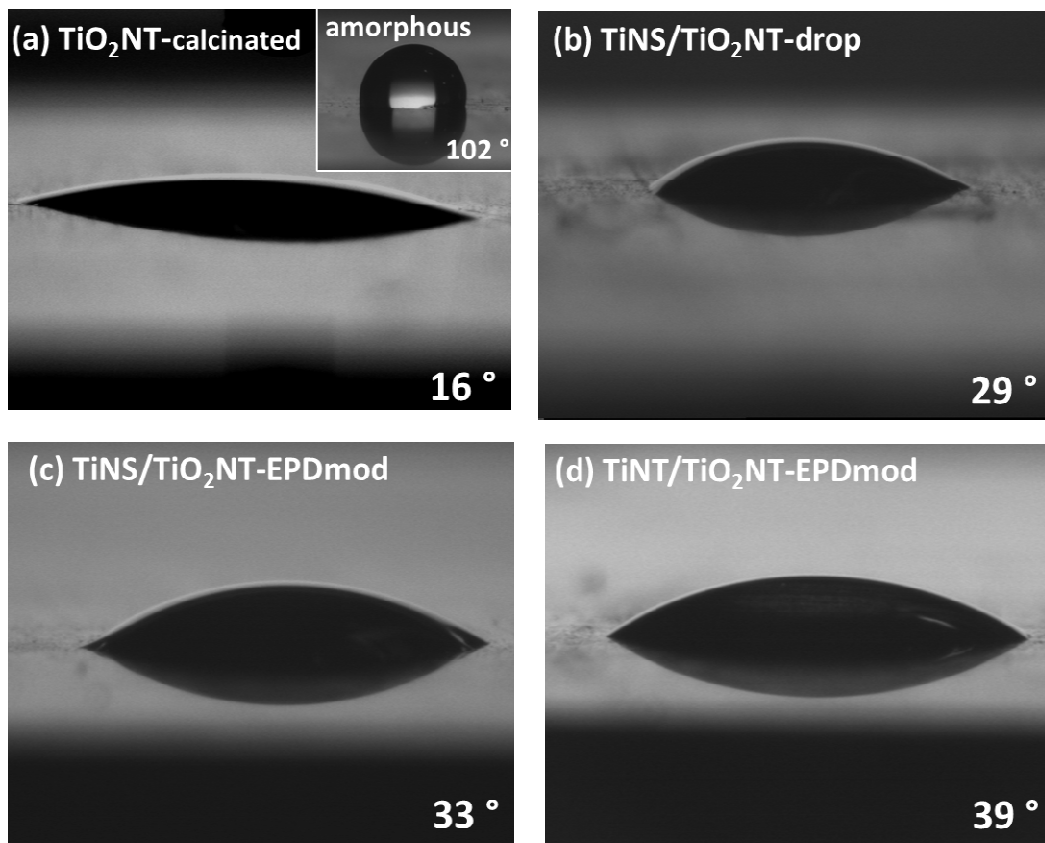


Figure 5: Contact angle images in water droplet on the surface of electrodes of (a) TiO_2NT calcinated and amorphous; (b) $\text{TiNS/TiO}_2\text{NT-drop}$; (c) $\text{TiNS/TiO}_2\text{NT-EPDmod}$ and (d) $\text{TiNT/TiO}_2\text{NT-EPDmod}$.

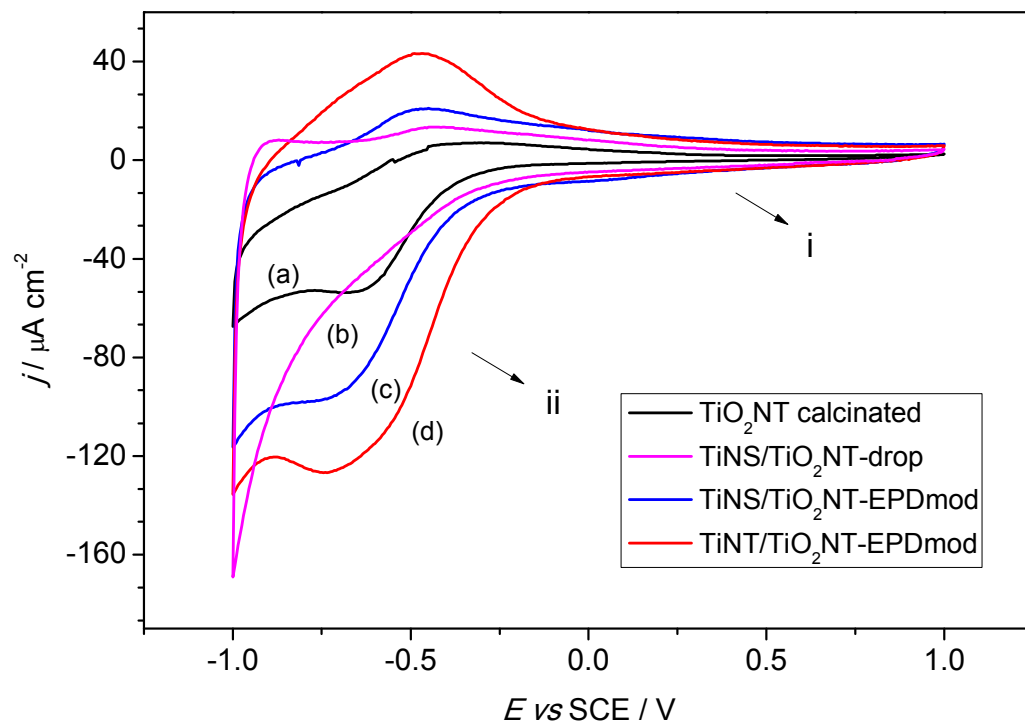


Figure 6: Cyclic voltammograms recorded for TiO₂ nanotubes electrodes in 0.1 mol L⁻¹ Na₂SO₄ at 25 °C; $dE/dt = 20 \text{ mV s}^{-1}$.

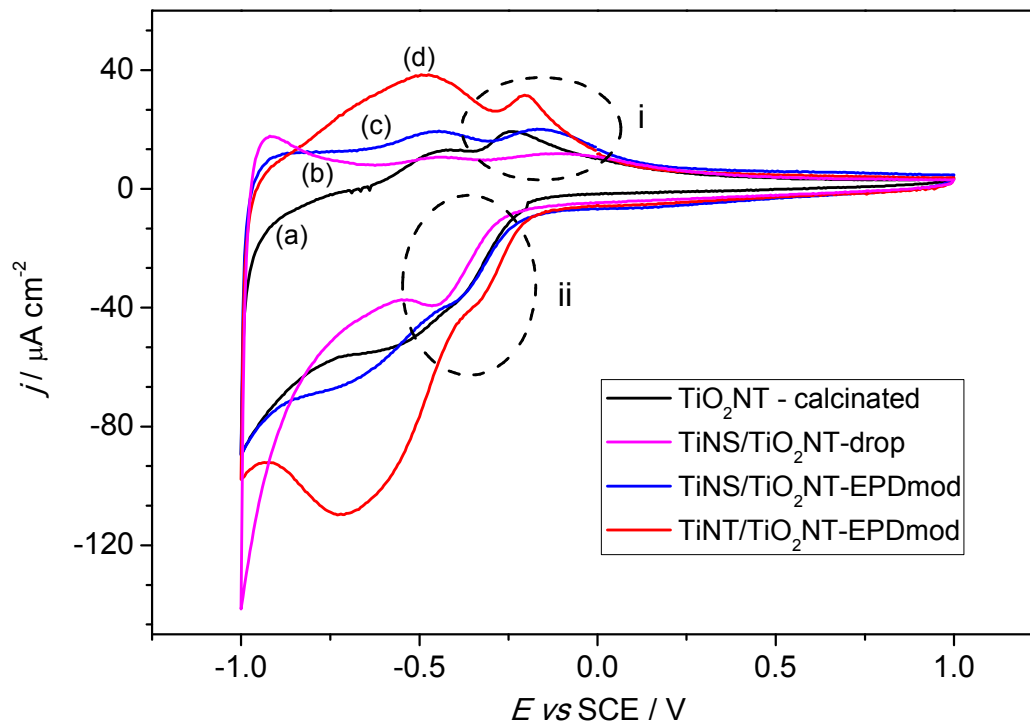


Figure 7: Cyclic voltammograms recorded for TiO_2 nanotubes electrodes in 0.025 mol L^{-1} methylene blue, MB in $0.1 \text{ mol L}^{-1} \text{ Na}_2\text{SO}_4$ at 25°C ; $dE/dt = 20 \text{ mV s}^{-1}$.